Enhanced Lifetime of Cyanine Salts in Dilute Matrix Luminescent Solar Concentrators via Counterion Tuning

Christopher K. Herrera[1], Aria Vahdani[2], Chenchen Yang[1], Matthew Bates[1], Sophia Y. Lunt[1,3], Babak Borhan[2], Richard R. Lunt[1,4,*]

[1]Department of Chemical Engineering and Materials Science, Michigan State University, East Lansing, Michigan 48824, United States

[2]Department of Chemistry, Michigan State University, East Lansing, Michigan 48824, United States

[3]Department of Biochemistry and Molecular Biology, Michigan State University, East Lansing, Michigan 48824, United States

[4]Department of Physics and Astronomy, Michigan State University, East Lansing, Michigan 48824, United States

ABSTRACT: Organic luminophores offer great potential for energy harvesting and light emission due to tunable spectral properties, strong luminescence, high solubility, and excellent wavelength-selectivity. To realize their full potential, the lifetimes of luminophores must extend to many years under illumination. Many organic luminophores, however, have a tendency to degrade and undergo rapid photobleaching, leading to the perception of intrinsic instability of organic molecules. In this work we demonstrate that by exchanging the counterion of a heptamethine cyanine salt the photostability and corresponding lifetime of dilute cyanine salts can be enhanced by orders of magnitude from 10 hours to an extrapolated lifetime of greater than 65,000 hours under illumination. To help correlate and comprehend the underlying mechanism behind this phenomenon, the water contact angle and binding energy of each pairing were measured and calculated. We find that increased water contact angle, and therefore increasing hydrophobicity, generally correlate to improved lifetimes. Similarly, a lower absolute binding energy between cation and anion correlates to increased lifetimes. Utilizing the binding energy formalism, we predict the stability of a new anion and experimentally verify with good consistency. Moving forward, these factors could be used to rapidly screen and identify highly photostable organic luminophore salt systems for a range of energy harvesting and light emitting applications.

Keywords: Organic salts, photostability, lifetime, luminescent solar concentrators

Introduction

Luminescent solar concentrators (LSCs) offer an inexpensive approach to large-area solar harvesting.[1–4] LSCs comprise luminophores dispersed in a waveguiding medium, where the luminophores absorb incident solar irradiance and reemit it in all directions (**Figure 1a**).[5] The majority of emitted photons are waveguided via total internal reflection to the edge-mounted photovoltaic (PV) cells. Due to the lack of transparent electrodes over the active layers, LSCs can be more easily designed for high-visible transparency applications like windows or mobile electronics by tuning the absorption and emission of the luminophore from the visible (VIS) into the near-infrared (NIR) (**Figure 1b**) or ultraviolet (UV) wavelength ranges.[6–15] Organic luminophores are excellent candidates due to wavelength-selective absorption through the UV, VIS, and NIR, high absorption coefficients, and high quantum yields (QY).[14,16–19]

Cyanine dyes, specifically NIR-absorbing heptamethine cyanines, (Cy7) are a class of cyanine derivatives that are commonly used for biomedical imaging and transparent LSCs due to their high molar extinction coefficients near the bandgap ($\varepsilon > 10^5$ M^{-1} cm^{-1}), low toxicity, and relatively high QY in the NIR (~20-30%).[14,20–28] The general cyanine structure consists of a conjugated heptamethine backbone, bound by two terminal heterocyclic indole groups, and a photoinactive counterion (**Figure 1c**). Despite the excellent optical properties, Cy7 is often observed to suffer from low photostability (on the order of hours under illumination) in a number of

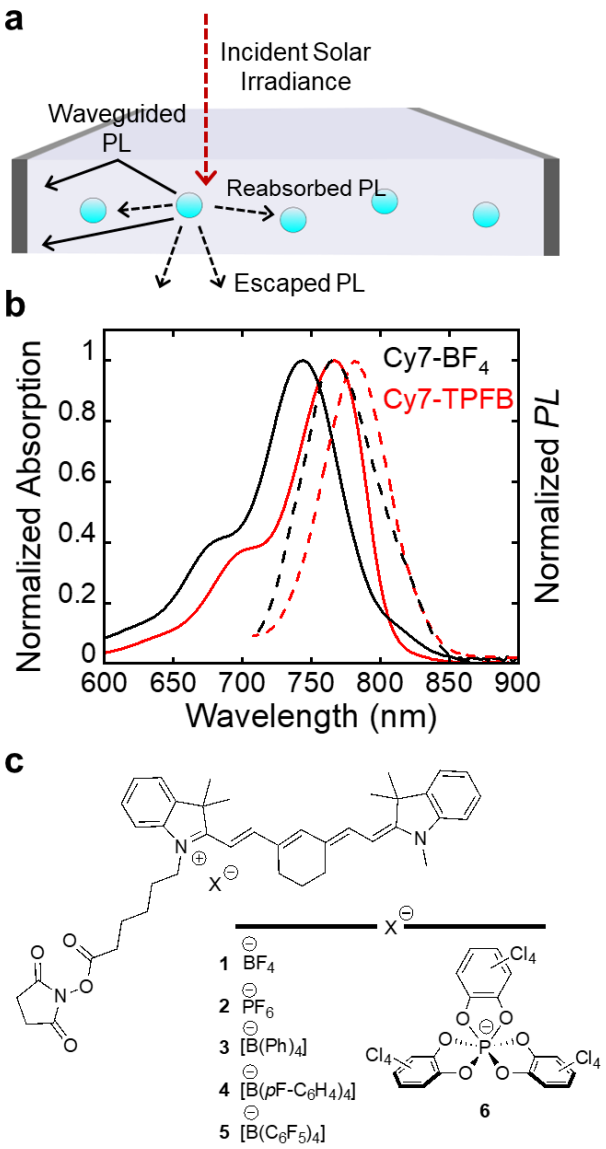

Figure 1. (a) A schematic of a luminescent solar concentrator where incident solar irradiance (red) is absorbed by a luminophore in the device. The light is then re-emitted in all directions where most will be waveguided to the edge-mounted solar cells (black, solid) via total internal reflection (TIR) while some light is lost to reabsorption or at angles too large for TIR. (b) The normalized absorption and emission spectra of two compounds in this study (Cy7-BF_4, Cy7-TPFB) are plotted. The narrow absorption and emission peak outside of the visible region of the solar spectrum. (c) The cationic heptamethine cyanine dye (Cy7) is paired with different anions listed below: (1) BF_4, (2) PF_6, (3) TRIS, (4) PhB, (5) FPhB, (6) TPFB.

demonstrated lifetime reports due to photobleaching.[29–35] Under illumination in ambient conditions, singlet oxygen is generated by reacting with the excited triplet states of Cy7, generating high energy species that cleave the heptamethine chain resulting in photobleaching.[20,24,31,36] This low photostability limits the potential of Cy7 as an effective luminophore for power-producing LSCs as the device is limited to the lifetime of the luminophore.[37] Recently, weakly coordinating anions have been shown to dramatically affect various properties such as solubility and thermal stability,[29,38,39] as well as modulating energy levels and voltages for neat film devices.[9,10,38,40–45] Weakly coordinating anions are known for being less nucleophilic than most anions due to a broader charge distribution. Moreover, we have previously demonstrated that the exchange of anions in heptamethine cyanine salts can result in extrapolated lifetimes of greater than 7 years in solid-state neat layers for organic photovoltaics without significantly altering the bandgap.[41] In those studies, improved device lifetime was shown to correlate to increased water contact angle and, thus, increased hydrophobicity. However, the close-packed environment is notably different than the dilute environment that luminophores commonly experience in LSCs (and imaging), which has properties more characteristic of a static solution. Additionally, the role of these anions in improving the photostability of organic salts is still not well understood, and it is difficult to determine how an anion will impact the salt.

In this work, we demonstrate that the lifetime under illumination of a commercial and a novel Cy7 luminophore in the dilute limit of an LSC can also be increased by orders of magnitude when only changing the anion (**Figure 1c**). We note that exchanging counterions has minimal impact to the optical properties of the luminophore (**Figure S1**). We evaluate the photostability through changes in luminophore absorption efficiency and the device quantum efficiency over time. Using these results, we further investigate potential correlating factors including hydrophobicity and ionic binding energy to inform selection and prediction of anions that will lead to further improved device lifetimes. By understanding the properties responsible for improving photostability, anions can be predicted, designed, and rapidly screened to further improve the lifetime of these luminophores.

Results and Discussion

We utilize a common commercially available imaging dye (Cy7 NHS ester) as the parent cation that can be representative of other cyanines and polymethines. We synthesized and tested an additional set of simpler hepthamethine cyanine salts with methyl groups in place of the NHS Ester chain around the amines (Cy7m-X). The parent cations were then ion exchanged with various weakly-coordinating anions

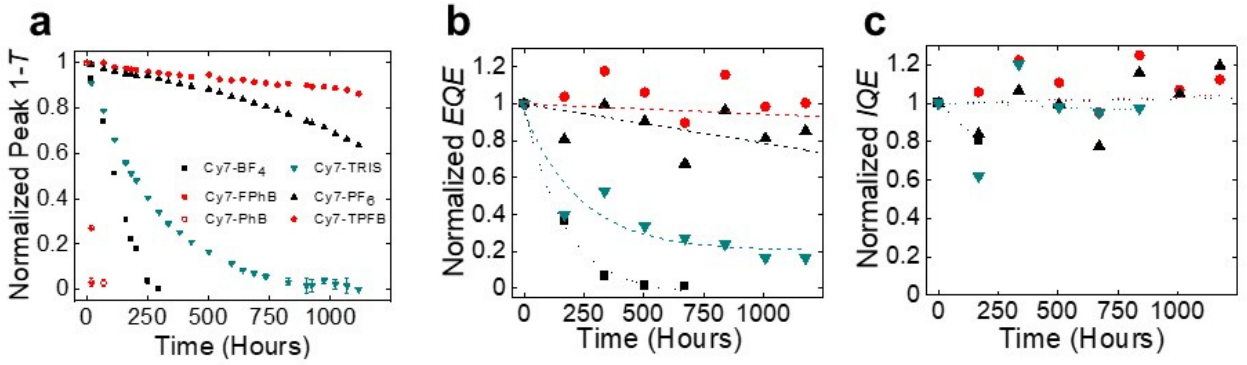

Figure 2. (a) The normalized 1-transmittance (T) for each Cy7-anion pairing is plotted vs time. T uncertainty is propagated from the equipment uncertainty of ±0.05%. (b) The corresponding normalized peak EQE for each device measured weakly is plotted against hours under illumination. Samples that degraded fully within a day were not included in the EQE dataset. (c) The calculated IQE from dividing the EQE by the normalized absorption is show vs time. The IQE is representative of QY, showing how the QY remains constant as the absorption decays.

as counterions including tetrafluoroborate (BF_4), tetrakis(pentfluorophenyl)borate (TPFB), hexafluorophosphate (PF_6), ΔTRISPHAT (TRIS), tetrakis(4-fluorophenyl)borate (FPhB), and tetraphenylborate (PhB). The counterion exchanges were confirmed via mass spectrometry (**Figure S2**). Importantly, to measure the intrinsic photostability and lifetime, Cy7-X pairings were encapsulated in a N_2 environment (< 1ppm H_2O and O_2) between two pieces of borosilicate glass and sealed with an epoxy. This method emulates a standard practice in window manufacturing of using inert gases to package materials susceptible to degradation (**Figure S3**)—for example, low-e Ag-based coatings in windows are packaged with Argon in part because this prevents optical degradation of the active Ag layer. Thus, leaks in the encapsulation are quickly apparent as the devices would fully quench within hours under illumination. Each salt had two 2"x2" encapsulated devices prepared for testing: one stored in the glovebox as a reference and the primary device that was tested under constant 1-sun illumination. We measured device transmittance (T) and external quantum efficiency (EQE_{LSC}) as a function of time to track changes in luminophore performance. Repeat devices were made in the cases of quick photodegradation (e.g. Cy7-PhB) to ensure the accuracy of the measurements (**Figure S4**). Because the voltage and fill factor of LSCs are largely dictated by the edge-mounted PV (which is not changing) the primary parameter that changes appreciably with time is the short-circuit current density (J_{sc}) due to changes in absorption and quantum yield (QY). Thus, the EQE (and the integrated EQE) can be used to proportionally track changes in J_{sc} (or relative changes in PCE) as:

$$J_{SC,LSC}^{int} = e \int EQE(\lambda) S(\lambda) d\lambda \qquad (1)$$

where S is the incident solar photon flux on the front surface of the LSC. By also tracking the absorption, we monitor the amount of photobleaching directly and can also determine changes in internal quantum efficiency (IQE), which is a good measure for changes in the QY as described below.

The EQE is defined as the ratio of the number of generated electrons to the total number of photons incident on the LSC waveguide front surface. The EQE of an LSC is defined as follows:

$$EQE_{LSC}(\lambda) = IQE_{LSC}(\lambda) \cdot \eta_{Abs}(\lambda) \qquad (2)$$

where η_{Abs} is the absorption efficiency and IQE_{LSC} is the internal quantum efficiency, ratio of generated electrons to the number of absorbed photons, of the LSC. This definition of EQE_{LSC} can be further defined as:

$$EQE_{LSC}(\lambda) = \eta_{ext}(\lambda) \cdot EQE_{PV} = (1 - R(\lambda)) \cdot \eta_{Abs}(\lambda) \cdot \eta_{PL} \cdot \eta_{Trap} \cdot \eta_{RA} \cdot EQE_{PV}^{*} \qquad (3)$$

where η_{ext} is the external optical efficiency, R is the front-surface reflectance, η_{PL} is the photoluminescence quantum yield (QY) of the luminophore, η_{Trap} is the waveguiding efficiency, η_{RA} is the reabsorption repression efficiency—dependent on the spectral overlap of the luminophore absorption and emission—and EQE_{PV}^{*} is the EQE of the edge-mounted PV at the emission of the luminophore. Therefore, the IQE_{LSC} is defined:

$$IQE_{LSC}(\lambda) = (1 - R(\lambda)) \cdot \eta_{PL} \cdot \eta_{Trap} \cdot \eta_{RA} \cdot EQE_{PV}^{*} \qquad (4)$$

Of these parameters, the reabsorption suppression and QY are luminophore properties. The remaining parameters are properties of the waveguide and the edge-mounted PV, neither of which will show changes with these time scales. Thus, changes in IQE translate directly as changes in QY. Because the edge-mounted PV typically has a lifetime > 20-25 years (e.g., Si), changes in EQE for an LSC will be dependent primarily

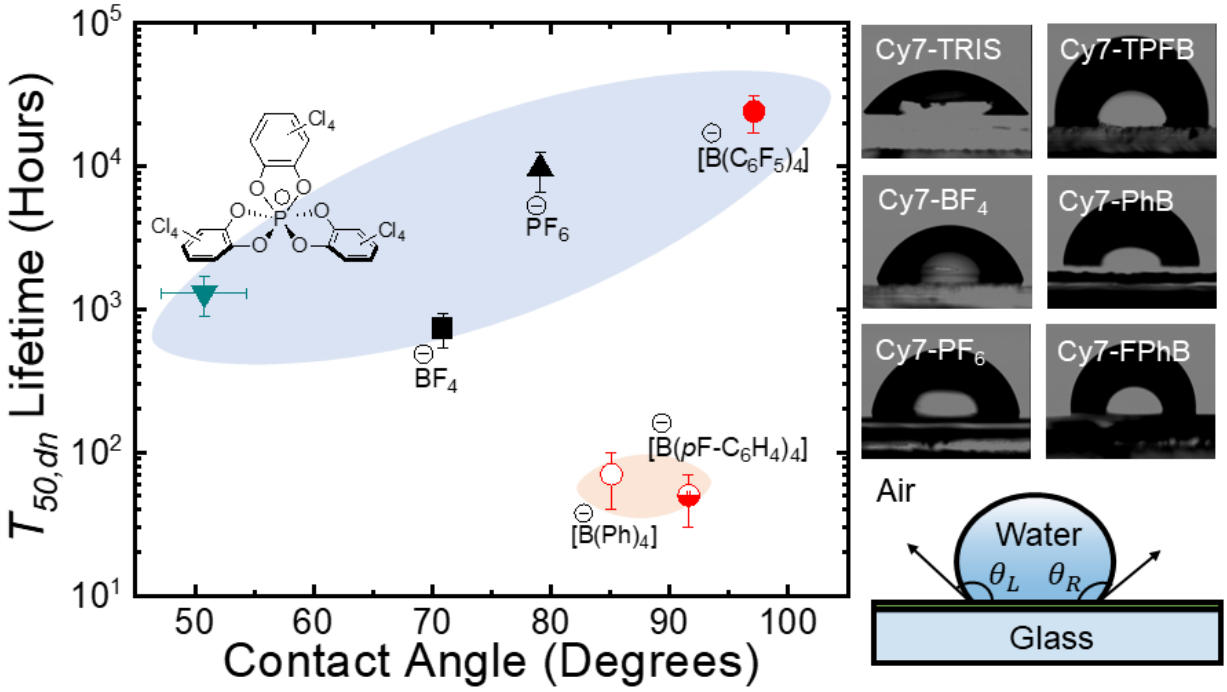

Figure 3. (left) Water contact angle vs $T_{50,dn}$ lifetime of each salt plotted on a semilogarithmic scale. Note that the lifetime was measured from dilute films while the contact angles are from neat films. An increase in lifetime can be correlated with an increase in hydrophobicity for anions that are completely halogen-terminated (blue ellipse) while anions that are fully or partially hydrogen-terminated do not show that correlation (orange ellipse). (right) Images used to calculate the water contact angle of each salt, taken 10 seconds after dropping the water onto the film.

on η_{Abs} and η_{PL} (or QY). There can be some changes in η_{RA} as the overall absorption decreases initially because there is strong overlap between absorption and PL for the polymethines, despite maintaining a relatively constant Stokes shift during photobleaching (**Figure S5**). The losses in absorption and QY dominate changes in EQE over time.

Lifetime can be characterized by T_{80} or T_{50}, which represent the operational time under constant illumination it takes for the device to reach 80% and 50% of its maximum output, respectively.[46] In **Figure 2a**, we show the variation of asborption (1-T) as a function of counterion pairing under constant 1-sun illumination. The absorption lifetime of Cy7 changes by many orders of magnitude. The EQE over time of each device is shown **Figure 2b** and shows similarly dramatic changes in the lifetime as a function of counterion, mirroring the trend of absorption loss. Notably Cy7-FPhB and Cy7-PhB are excluded from EQE because they were completely photobleached within one day (**Figure S6**). The absorption and EQE peaks (and in turn, the integrated J_{sc}, **Figure S7**) decay exponentially with time until they approach 0 (**Figure S8**), making the lifetime a parameter that can be reasonably extrapolated to represent total lifetime under standard day/night cycles ($T_{50,dn}$) by multiplying the measured values by 5.6 (that is, on average in the U.S. there are 5.6hr of 1-Sun illumination). We use the term $T_{50,dn}$ interchangeably with lifetime for the remainder of this work. Of the Cy7-X series, Cy7-TPFB demonstrates the highest photostability with 4200 ± 1200 hrs under constant 1-sun illumination ($T_{50,dn}$ = 24,000 ± 7,000 hrs). Cy7-PF_6 also demonstrates a lifetime of greater than 1700 ± 530 hrs ($T_{50,dn}$ = 9,700 ± 3,000 hrs), which is comparable but significantly lower than Cy7-TPFB. Cy7-TRIS and Cy7-BF_4 exhibit lifetimes 230 ± 70 hrs ($T_{50,dn}$ = 1,300 ± 400 hrs) and 120 ± 40 hrs ($T_{50,dn}$ = 700 ± 200 hrs), respectively. Cy7-PhB and Cy7-FPhB demonstrate lifetimes below 20 hrs. The consistency between absorption loss and EQE loss indicate that ratio between IQE and QY should be constant and that the primary degradation mechanism is bleaching of the absorption. To confirm this, we look at the IQE directly in **Figure 2c**. Indeed, we find that the IQE stays essentially constant for each material until it is fully degraded. Thus, the degradation of the luminophore and device can be adequately described by losses in absorption in these materials.

The measured and extrapolated lifetime results are summarized in **Table 1**. We note that the trends here for Cy7 cation are similar for the simpler Cy7m that lacks the NHS Ester group (replaced with a methyl group, see **Figure S9**). Cy7m-I has a lifetime of 47 hrs ± 10 hrs ($T_{50,dn}$ = 240 ± 80 hrs) while Cy7m-TPFB has an extrapolated lifetime of 11,600 ± 2,800 hrs ($T_{50,dn}$ =

65,000 ± 16,000 hrs), a similarly dramatic improvement like Cy7-TPFB (**Figure S10**). By replacing the NHS Ester chain with a simple methyl group, the lifetime of Cy7 increases by a factor of > 2.5.

In our previous investigation on the effect of anion exchange on the lifetime of an organic salt photovoltaic, we found that water contact angle was the only parameter (of many investigated) that showed any correlation with the operating lifetime of the device, suggesting that increased hydrophobicity of the salt layer was indicative of improved lifetime. We tested if this macroscopic property, measured on neat films of each salt, would be consistent with lifetime differences observed in a dilute environment. Figure 3 shows the measured water contact angles plotted against lifetime for each salt. Notably, Cy7-PhB and Cy7-FPhB showed much lower lifetimes (on the order of 10s of hrs) compared to the other salts despite having high water contact angles. A key distinctive factor for PhB and FPhB is that they are primarily hydrogen-terminated. When delineating between fully halogen-terminated and partially halogenated anions, the halogenated anions show a trend that resembles the result in previous work. While the water contact angle may prove helpful in thinking about the impact and the potential factors of degradation for how the various anions will compare to others, it does not fully capture the trends in a universal way.

Table 1. Extrapolated Lifetime of Each Salt. T_{80} and T_{50} are measured from the normalized 1-T plot (except for Cy7-TPFB and Cy7m-TPFB, which required extrapolation for T_{50}). $T_{50,dn}$ is the device lifetime adjusted for the average day-night cycles in the US.

Salt	T_{80} (Hours)	T_{50} (Hours)	$T_{50,dn}$ (Hours)
Cy7-BF_4	52 ± 14	120 ± 40	700 ± 200
Cy7-PF_6	690 ± 190	1,700 ± 530	9,700 ± 3,000
Cy7-TRIS	92 ± 27	230 ± 70	1,300 ± 400
Cy7-FPhB	4 ± 1	10 ± 4	60 ± 20
Cy7-PhB	5 ± 2	12 ± 5	70 ± 30
Cy7-TPFB	1,710 ± 490	4,200 ± 1,200	24,000 ± 7,000
Cy7m-I	16 ± 5	47 ± 10	240 ± 80
Cy7m-TPFB	4,600 ± 1,100	11,600 ± 2,800	65,000 ± 16,000

Based on the idea that the water contact angle might be elucidating some aspect of the underlying ionic bonding arrangement, we explored the ionic binding energy via molecular DFT simulations.

For these calculations, we utilized a local density approximation functional (LDA-PWC) and the DNP 3.5 basis set in the DMol3 package in Materials Studio.[47,48] LDA has been reported to provide good results for non-covalent interactions and has been shown to provide good results with PWC/DNP in binding energy calculations between ligands and protein binding sites.[49–51] Using DFT to study this isolated cation-anion pairings is more suitable to describe the system in comparison to the bulk film study of contact angle measurements because the salts are contained in the dilute environment rather than a close-packed neat layer. The binding energies are calculated as follows:

$$E_B = E_{cat+an} - (E_{cat} + E_{an}) \quad (5)$$

where E_B is the binding energy between Cy7 and a given anion, E_{cat+an} is the minimized system energy of Cy7 coordinated with the same anion (**Figure 4a**), E_{cat} is the minimized energy of just Cy7, and E_{an} is the minimized energy of just the anion. The anion was simulated in initial positions around the cation (**Figure S11**) and the system was energy minimized to ensure that the ions were conformed optimally. **Figure 4b** shows the minimum calculated binding energy plotted against device lifetime. Between anions of similar structures, there is a correlation between weaker binding energy and increasing device lifetime. We use a linear fit on the semi-logarithmic plot to describe the relationship of binding energy to the device lifetime between anions of a similar size—such as the phenylborate anions. Compared to the water contact angle trends, the trends with binding energy appear to be grouped more meaningfully and with more consistent trendlines between groupings even if it is it still not yet universal. Between the two anion size categories, the fit lines demonstrate similar slopes; however, the larger conjugated anions shift the lifetime trend upward compared to the small, hard anions (PF_6 and BF_4), suggesting that larger anion size can contribute to improved photostability despite having stronger binding energies than the smaller anions. Interestingly, the trendline defined by TPFB, FPhB, and PhB, suggests that the increased number of F atoms improves lifetime through a broadening of the charge distribution. Given the symmetrical nature of the anions presented in this work with halogens evenly distributed along all terminal bonds, this draws the charge towards the edges of the anion.

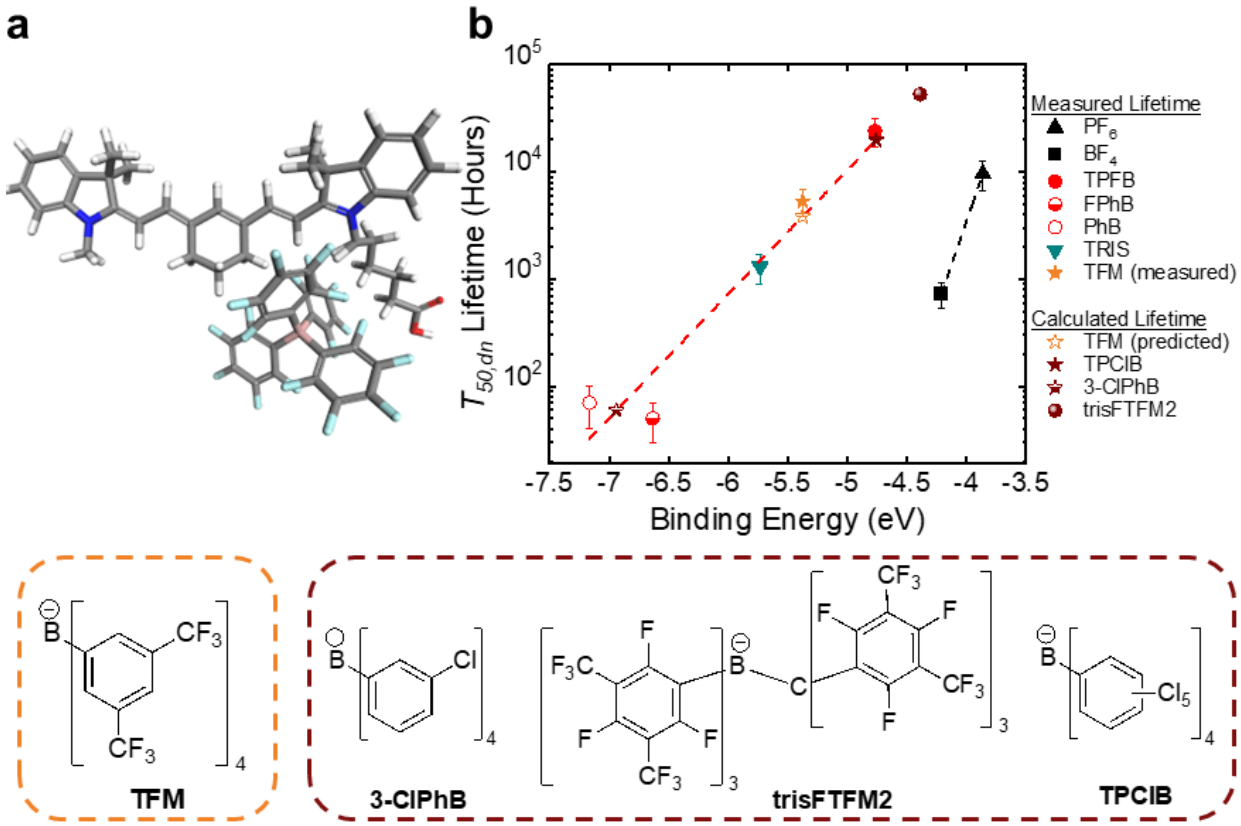

Figure 4. (a) A representative Cy7 was simulated in Materials Studio with a carboxylic acid-terminated chain. Each anion was simulated with the cation with 5 potential initial positions prior to geometric optimization. Depicted here is the representative Cy7 with TPFB in the energetically minimized position. (b) The minimum binding energy from any of the anion positions is plotted against the $T_{50,dn}$ lifetime. Anions with similar structures were used to generate fit lines. The phenyl borate anions were used to predict the lifetime of Cy7 coordinated with tetrakis[3,5-bis(trifluoromethyl)phenyl]borate (TFM, open star) and is then compared to the experimentally determined lifetime (closed star), showing good agreement. Additional lifetimes are predicted for other anions. Structures of TFM (orange dashed box) and other theoretical anions (brown dashed box) are displayed.

From the simulations, the most favorable position for the counterion to position itself was always around the amine bonded with the carboxylic acid chain (e.g. **Figure 4a**). The electron-withdrawing characteristics from the carboxylic acid group alter the charge distribution on Cy7, making the amine that it is bonded to more positively charged. This positive charge makes the amine a more susceptible site for a degradation reaction to occur but also electrostatically attracts the counterion to a greater extent. Given that we have identified the combination of anion size and broader charge distribution (from electronegative halogens) as factors that lead to improved photostability, it is likely that the anion acts to shield the charge upon coordination, by creating a barrier for degradation agents (similar to oxygen interacting with the labile polymethine chain, disrupting conjugation) and increasing the overall lifetime. Specifically, the delocalization of the charge in the anion can result in stronger electrostatic interactions with potential degradation agents, which can work in combination with the increased size to improve protection of the labile sites. The weaker binding energy could allow for the anion to experience an increased range of mobility to protect other labile sites from degradation. In this experiment, the cyanine salts were encapsulated in a nitrogen environment to ensure that superoxide and singlet oxygen would be unlikely contributors in degradation. Relative to Cy7m-TPFB to Cy7-TPFB, the lifetime further increases by a factor of ~2.7, indicating that the NHS ester chain has some involvement in the degradation of Cy7 (after the primary mechanism is reduced via improved counterions). The Cy7 salts are contained in a matrix that retains some of the butyl methacrylate monomers which have an ester group capable of interacting with the photoexcited-state of the Cy7 cation.

We use our fitted trend with binding energy to predict the lifetime of another large anion: tetrakis(3,5-bis(trifluoromethyl)phenyl)borate (TFM) (**Figure 4b**). TFM occupies more space having more fluorine atoms than TPFB due to its trifluoromethyl groups. Furthermore, we also used it to further understand how factors such as size and nature of the halogen impacts lifetime. We calculate a binding energy of this system of approximately -5.4 eV, resulting in a predicted lifetime of ~3800 hrs when using the previous fit. Cy7-TFM was then synthesized, and the lifetime measured. The $T_{50,dn}$ of a Cy7-TFM blend was 5300 ± 1500 hrs (**Figure S12**), which shows remarkably close agreement (within error) to the predicted value. Cy7-TFM has a lower lifetime and stronger binding energy than Cy7-TPFB, so while size and number of halogen atoms do play a role, the addition of hydrogen-terminated positions in the Cy7-TFM can contribute to a larger binding energy and reducing the overall lifetime. Using these tools, it might be possible to screen for anions leading to the highest probability of long lifetime. (**Figure 4b**). Changing the F atoms to Cl in TPFB does not significantly change the binding energy. However, increasing the anion size by adding additional rings (e.g. forming trisFTFM2) is found to result in a weaker binding energy of -4.38 eV and, therefore, a higher predicted $T_{50,dn}$ of 53,000 hrs with the Cy7 cation that would more than double the lifetime (**Figure 4b**). Extrapolating this to hypothetical Cy7m-trisFTFM2, lifetimes up to 140,000 hrs may be possible.

Conclusions

In conclusion, we have demonstrated how counterion selection can dramatically increase the lifetime of luminescent heptamethine salts from hours to >20,000 hrs, even at the dilute limit. By monitoring the lifetime via luminophore absorption and photocurrent generation, we were able to identify that device degradation was a result of photobleaching. The lifetime was improved for the Cy7-TPFB pairing by removing the NHS ester chain in favor of a methyl group, resulting in an extrapolated lifetime of >65,000 hrs. Using water contact angle measurements, we show that increasing hydrophobicity and extent of halogenation (reduced protonation) results in increased lifetime in the dilute state. We further calculate the binding energies of the salt pairings and show an improved correlation with lifetime, where weaker ion binding energies for large anions correspond to increased lifetimes. This binding energy correlation was then used to predict the lifetime of additional anions. Finally, in chromophores not synthesized in this study, we predict anion targets that possess potential for exceptionally long lifetime. This work ultimately demonstrates that even seemingly "unstable" organic salt luminophores can be made highly "stable" by means of simple counterion exchange. This study also has the potential to provide a more viable pathway to the design of organic luminophore salts, providing them with greater commercial viability in a wider range of highly demanding energy and imaging applications.

Materials and Methods

Materials. Cyanine7 NHS ester (Cy7) was purchased from Lumiprobe and is initially paired with tetrafluoroborate (BF_4) during synthesis. Potassium tetrakis(pentfluorophenyl)borate (abbreviated as K-TPFB) was purchased from Boulder Scientific Company; Tetrabutylammonium Δ-tris(tetrachloro-1,2benzenediolato)phosphate(V) (TBA-TRIS), Sodium tetrakis(4-fluorophenyl)borate dihydrate (Na-FPhB), Sodium hexafluorophosphate (Na-PF_6), Sodium tetraphenylborate (Na-PhB) were purchased from Sigma Aldrich. The Shandon Mount, the acting waveguiding media, was purchased from ThermoFisher Scientific.

Counterion Exchange. Counterion exchange was performed following the procedure described in source.[9] The standard Cy7 salt and each counterion precursor were massed in a 1:2 molar ratio and dissolved into a solution of 6:1 volumetric ratio of dichloromethane to methanol. The solution was covered and stirred at room temperature for approximately 1 hour. The products were then passed through a silica gel column with dichloromethane. The colored solution is collected, and the solvent is evaporated until dry, and the powder product is collected.

Mass Spectrometry. The exchanged salts were analyzed using a high resolution ultra high-performance liquid chromatography mass spectrometry (UHPLC-MS) system, Waters Xevo G2-XS QTof. The salts were dissolved into solvent mixtures with HPLC-grade 1:9 dichloromethane:acetonitrile at concentrations of 1 μM, 100 nM, and 10nM. Samples were scanned in positive and negative mode to verify the exchange (**Figure S2**). A blank solution was run between each scan to prevent previous scans from affecting the results. The column temperature was set to 30 °C, and the flow rate was 0.2 mL/min using 100% acetonitrile as the mobile solvent.

Device Fabrication. Salts were dispersed into ethanol with a concentration around 0.125 mg/mL. Solutions were mixed with the Shandon mount with a volumetric ratio of 1:2 respectively. 3 mL of this mixture was then drop-cast onto a 2" x 2" glass substrate and left to dry for 4 hours in a N_2 environment (< 1 ppm O_2 and H_2O). After drying, epoxy was applied around the border of the Shandon film. An identical 2" x 2" glass piece was pressed against the epoxy, ensuring there are no air channels

in the epoxy that allow for gas to reach the rest of the Shandon film. The active area inside the epoxy is masked with black paper; the epoxy is then UV-treated while the device is in N_2.

Lifetime Testing. Two sets of encapsulated devices were made with one 2"x2" device per Cy7-counterion pairing in each set. One set of encapsulated devices was held under constant 1-sun illumination (Chameleon Sulfur Plasma lamp). The other set of devices was kept in a N_2 environment in the dark as a reference for the photodegradation of the exposed devices. The transmission (*T*) spectra were measured using a Perkin-Elmer Lambda 800 UV-VIS Spectrometer. For the devices held under constant illumination, *T* measurements were taken daily for the first 10 days then once every three days for the long lifetime salts (after shorter lifetime salts completely degraded) to track changes in luminophore absorption. For the *EQE* measurement, three edges of the panels were colored black and covered by black tape to more accurately measure the *EQE* from a single edge-mounted PV.[52] The uncovered side was mounted with a laser-cut silicon solar cell using index-matching gel. The *EQE* was measured using a monochromatic excitation source that was positionally confined to the center of the device using an optical fiber. The *EQE* of each sample was taken weekly from 300-900nm. The peaks of the *EQE* and 1-*T* were plotted against hours under illumination to show degradation of the salts vs time.

Water Contact Angle Measurements. Films of each of the salts were deposited via spincoating. Each salt was dissolved into 3:1 dichloromethane to chlorobenzene mixture at a concentration of 10 mg/mL. The solutions were deposited onto plasma-cleaned glass substrates, and the substrates were spun at 2000rpm for 30 seconds. A drop of water was placed onto the substrate and an image was captured of the drop 10 seconds after it contacted the substrate. The Krüss Drop Shape Analyzer was used measure the contact angle of the water and the salt film.

Binding Energy Calculations. A simplified cyanine molecule with the NHS Ester group removed and the ligand terminated with a carboxyl group was generated in Materials Studio along each anion. Conformation of the ions were calculated using the DMol3 software package of Materials Studio with the LDA-PWC functional using the DNP 3.5 basis set. A dispersion correction (DFT-D) was applied with OBS custom method. K-point separation was set to 0.07 $Å^{-1}$, and the energy cutoff was set to 700 eV. Task quality, integration accuracy, and SCF tolerance were set to "Fine."

Tasks were executed with each ion individually first. First, the conformation of each ion was calculated using the "Geometry Optimization" task with an energy tolerance of 1e-5 Ha. The minimum energy was then calculated with the "Energy" task. Each anion was put in the same simulation space as the simplified Cy7 cation using 5 initial starting positions (Figure S4). In each position, the anion was rotated to minimize energy. The "Geometry Optimization" task was again performed on the cation-anion system to ensure optimal atom positioning. The energy of the system at each position was then calculated. The energies of the cation and anion isolated systems were subtracted from the lowest system energy of the pairing to determine the binding energy of the system.

AUTHOR INFORMATION

Corresponding Author

Richard R. Lunt - Department of Chemical Engineering and Materials Science, East Lansing, Michigan 48824, United States; Department of Physics and Astronomy, Michigan State University, East Lansing, Michigan 48824, United States

Email: rlunt@egr.msu.edu

Authors

Christopher K. Herrera - Department of Chemical Engineering and Materials Science, East Lansing, Michigan 48824, United States

Aria Vahdani- Department of Chemistry, East Lansing, Michigan 48824, United States

Chenchen Yang - Department of Chemical Engineering and Materials Science, East Lansing, Michigan 48824, United States

Matthew Bates - Department of Chemical Engineering and Materials Science, East Lansing, Michigan 48824, United States

Sophia Y. Lunt – Department of Biochemistry, East Lansing, Michigan 48824, United States; Department of Chemical Engineering and Materials Science, East Lansing, Michigan 48824, United States

Babak Borhan – Department of Chemistry, East Lansing, Michigan 48824, United States

CONFLICT OF INTEREST

R.R.L. is a founder and non-majority owner of Ubiquitous Energy, Inc., a company working to commercialize TPV and TLSC technologies. A patent based on this work has been filed by C.K.H, A. V., B.B., and R.R.L. C.Y., M.B., and S.Y.L. have no conflicts of interest.

FUNDING SOURCES

The authors thank Ubiquitous Energy Inc for financial support of this work and thank Michigan State University (MSU) Strategic Partnership Grants and the Climate Change Research Support Program Seed Grant for partial support of this work. C.K.H. and S.Y.L. acknowledge support from the National Science

Foundation under CAREER Grant No. CBET 1845006. S.Y.L. was further supported by the National Cancer Institute of the National Institutes of Health under Award Number R01CA270136 and the National Institute of Environmental Health Sciences of the National Institutes of Health under Award Number R01ES030695.

ACKNOWLEDGEMENTS

The authors also thank the MSU Mass Spectrometry and Metabolomics Core.

SUPPORTING INFORMATION

The Supporting Information is available free of charge at XX.

Device transmittance and EQE spectra over time; lifetime for additional cations and anions, simulation details, and mass spectrometry data.

REFERENCES

(1) Traverse, C. J.; Pandey, R.; Barr, M. C.; Lunt, R. R. Emergence of Highly Transparent Photovoltaics for Distributed Applications. *Nat. Energy* **2017**, *2*, 849-860.

(2) Yang, C. C.; Liu, D. Y.; Rennya, A.; Kuttipillai, P. S.; Lunt, R. R. Integration of Near-Infrared Harvesting Transparent Luminescent Solar Concentrators onto Arbitrary Surfaces. *J. Lumin.* **2019**, *210*, 239–246.

(3) Mansour, A. F.; El-Shaarawy, M. G.; El-Bashir, S. M.; El-Mansy, M. K.; Hammam, M. A Qualitative Study and Field Performance for a Fluorescent Solar Collector. *Polym. Test.* **2002**, *21*, 277–281.

(4) Debije, M. G.; Verbunt, P. P. Thirty Years of Luminescent Solar Concentrator Research: Solar Energy for the Built Environment. *Adv. Energy Mater.* **2012**, *2*, 12–35.

(5) Li, Y.; Sun, Y.; Zhang, Y.; Dong, W.-J. Improving the Photostability of Printed Organic Photovoltaics through Luminescent Solar Concentrators. *Opt. Mater.* **2020**, *108*, 110194.

(6) Husain, A. A. F.; Hasan, W. Z. W.; Shafie, S.; Hamidon, M. N.; Pandey, S. S. A Review of Transparent Solar Photovoltaic Technologies. *Renew. Sustain. Energy Rev.* **2018**, *94*, 779–791.

(7) Lunt, R. R. Theoretical Limits for Visibly Transparent Photovoltaics. *Appl. Phys. Lett.* **2012**, *101*, 043902.

(8) Lunt, R. R.; Bulovic, V. Transparent, near-Infrared Organic Photovoltaic Solar Cells for Window and Energy-Scavenging Applications. *Appl. Phys. Lett.* **2011**, *98*, 113305.

(9) Suddard-Bangsund, J.; Traverse, C. J.; Young, M.; Patrick, T. J.; Zhao, Y.; Lunt, R. R. Organic Salts as a Route to Energy Level Control in Low Bandgap, High Open-Circuit Voltage Organic and Transparent Solar Cells That Approach the Excitonic Voltage Limit. *Adv. Energy Mater.* **2016**, *6*, 1501659.

(10) Traverse, C. J.; Young, M.; Suddard-Bangsund, J.; Patrick, T.; Bates, M.; Chen, P.; Wingate, B.; Lunt, S. Y.; Anctil, A.; Lunt, R. R. Anions for Near-Infrared Selective Organic Salt Photovoltaics. *Sci. Rep.* **2017**, *7*, 16399.

(11) Veron, A. C.; Zhang, H.; Linden, A.; Nuesch, F.; Heier, J.; Hany, R.; Geiger, T. NIR-Absorbing Heptamethine Dyes with Tailor-Made Counterions for Application in Light to Energy Conversion. *Org. Lett.* **2014**, *16*, 1044–1047.

(12) Yang, C. C.; Lunt, R. R. Limits of Visibly Transparent Luminescent Solar Concentrators. *Adv. Opt. Mater.* **2017**, *5*, 1600851.

(13) Zhao, Y.; Lunt, R. R. Transparent Luminescent Solar Concentrators for Large-Area Solar Windows Enabled by Massive Stokes-Shift Nanocluster Phosphors. *Adv. Energy Mater.* **2013**, *3*, 1143–1148.

(14) Zhao, Y. M.; Meek, G. A.; Levine, B. G.; Lunt, R. R. Near-Infrared Harvesting Transparent Luminescent Solar Concentrators. *Adv. Opt. Mater.* **2014**, *2*, 606–611.

(15) Albano, G.; Colli, T.; Nucci, L.; Charaf, R.; Biver, T.; Pucci, A.; Aronica, L. A. Synthesis of New Bis[1-(Thiophenyl)Propynones] as Potential Organic Dyes for Colorless Luminescent Solar Concentrators (LSCs). *Dyes Pigments* **2020**, *174*, 108100.

(16) Yang, C.; Sheng, W.; Moemeni, M.; Bates, M.; Herrera, C. K.; Borhan, B.; Lunt, R. R. Ultraviolet and Near-Infrared Dual-Band Selective-Harvesting Transparent Luminescent Solar Concentrators. *Adv. Energy Mater.* **2021**, *11*, 2003581.

(17) Yang, C.; Moemeni, M.; Bates, M.; Sheng, W.; Borhan, B.; Lunt, R. R. High-Performance Near-Infrared Harvesting Transparent Luminescent Solar Concentrators. *Adv. Opt. Mater.* **2020**, *8*, 1901536.

(18) Banal, J. L.; Zhang, B.; Jones, D. J.; Ghiggino, K. P.; Wong, W. W. H. Emissive Molecular Aggregates and Energy Migration in Luminescent Solar Concentrators. *Acc. Chem. Res.* **2017**, *50*, 49–57.

(19) Sala, P. D.; Buccheri, N.; Sanzone, A.; Sassi, M.; Neri, P.; Talotta, C.; Rocco, A.; Pinchetti, V.; Beverina, L.; Brovelli, S.; Gaeta, C. First Demonstration of the Use of Very Large Stokes Shift Cycloparaphenylenes as

Promising Organic Luminophores for Transparent Luminescent Solar Concentrators. *Chem. Commun.* **2019**, *55*, 3160–3163.

(20) Nani, R. R.; Kelley, J. A.; Ivanic, J.; Schnermann, M. J. Reactive Species Involved in the Regioselective Photooxidation of Heptamethine Cyanines. *Chem. Sci.* **2015**, *6*, 6556–6563.

(21) Sato, K.; Gorka, A. P.; Nagaya, T.; Michie, M. S.; Nakamura, Y.; Nani, R. R.; Coble, V. L.; Vasalatiy, O. V.; Swenson, R. E.; Choyke, P. L.; Schnermann, M. J.; Kobayashi, H. Effect of Charge Localization on the in Vivo Optical Imaging Properties of Near-Infrared Cyanine Dye/Monoclonal Antibody Conjugates. *Mol. Biosyst.* **2016**, *12*, 3046–3056.

(22) Mishra, A.; Behera, R. K.; Behera, P. K.; Mishra, B. K.; Behera, G. B. Cyanines during the 1990s: A Review. *Chem. Rev.* **2000**, *100*, 1973–2012.

(23) Gorka, A. P.; Nani, R. R.; Schnermann, M. J. Harnessing Cyanine Reactivity for Optical Imaging and Drug Delivery. *Acc. Chem. Res.* **2018**, *51*, 3226–3235.

(24) Gorka, A. P.; Nani, R. R.; Zhu, J. J.; Mackem, S.; Schnermann, M. J. A Near-IR Uncaging Strategy Based on Cyanine Photochemistry. *J. Am. Chem. Soc.* **2014**, *136*, 14153–14159.

(25) Michie, M. S.; Gotz, R.; Franke, C.; Bowler, M.; Kumari, N.; Magidson, V.; Levitus, M.; Loncarek, J.; Sauer, M.; Schnermann, M. J. Cyanine Conformational Restraint in the Far-Red Range. *J. Am. Chem. Soc.* **2017**, *139*, 12406–12409.

(26) Ma, X. M.; Hua, J. L.; Wu, W. J.; Jin, Y. H.; Meng, F. S.; Zhan, W. H.; Tian, H. A High-Efficiency Cyanine Dye for Dye-Sensitized Solar Cells. *Tetrahedron* **2008**, *64*, 345–350.

(27) Alford, R.; Simpson, H. M.; Duberman, J.; Hill, G. C.; Ogawa, M.; Regino, C.; Kobayashi, H.; Choyke, P. L. Toxicity of Organic Fluorophores Used in Molecular Imaging: Literature Review. *Mol. Imaging* **2009**, *8*, 341-354.

(28) Li, D.-H.; Schreiber, C. L.; Smith, B. D. Sterically Shielded Heptamethine Cyanine Dyes for Bioconjugation and High Performance Near-Infrared Fluorescence Imaging. *Angew. Chem. Int. Ed.* **2020**, *59*, 12154–12161.

(29) Woo, S. W.; Kim, J. Y.; Hwang, T. G.; Lee, J. M.; Kim, H. M.; Namgoong, J.; Yuk, S. B.; Kim, J. P. Effect of Weakly Coordinating Anions on Photo-Stability Enhancement of Basic Dyes in Organic Solvents. *Dyes Pigments* **2019**, *160*, 765–771.

(30) Bouit, P. A.; Di Piazza, E.; Rigaut, S.; Le Guennic, B.; Aronica, C.; Toupet, L.; Andraud, C.; Maury, O. Stable Near-Infrared Anionic Polymethine Dyes: Structure, Photophysical, and Redox Properties. *Org. Lett.* **2008**, *10*, 4159–4162.

(31) Chen, P.; Sun, S. Q.; Hu, Y. F.; Qian, Z. G.; Zheng, D. S. Structure and Solvent Effect on the Photostability of Indolenine Cyanine Dyes. *Dyes Pigments* **1999**, *41*, 227–231.

(32) Funabiki, K.; Yagi, K.; Nomoto, M.; Kubota, Y.; Matsui, M. Improvement of the Thermal Stability of Near-Infrared-Absorbing Heptamethinecyanine Dyes by Anion-Exchange from an Iodide to Fluorine-Containing Anions. *J. Fluor. Chem*. **2015**, *174*, 132–136.

(33) Funabiki, K.; Yagi, K.; Ueta, M.; Nakajima, M.; Horiuchi, M.; Kubota, Y.; Mastui, M. Rational Molecular Design and Synthesis of Highly Thermo- and Photostable Near-Infrared-Absorbing Heptamethine Cyanine Dyes with the Use of Fluorine Atoms. *Chem.- Eur. J.* **2016**, *22*, 12282–12285.

(34) Renikuntla, B. R.; Rose, H. C.; Eldo, J.; Waggoner, A. S.; Armitage, B. A. Improved Photostability and Fluorescence Properties through Polyfluorination of a Cyanine Dye. *Org. Lett.* **2004**, *6*, 909–912.

(35) Samanta, A.; Vendrell, M.; Das, R.; Chang, Y. T. Development of Photostable Near-Infrared Cyanine Dyes. *Chem. Commun.* **2010**, *46*, 7406–7408.

(36) Kanofsky, J. R.; Sima, P. D. Structural and Environmental Requirements for Quenching of Singlet Oxygen by Cyanine Dyes. *Photochem. Photobiol.* **2000**, *71*, 361–368.

(37) Delgado-Sanchez, J. M. Luminescent Solar Concentrators: Photo-Stability Analysis and Long-Term Perspectives. *Sol. Energy Mater. Sol. Cells* **2019**, *202*, 110134.

(38) Kim, J. Y.; Hwang, T. G.; Woo, S. W.; Lee, J. M.; Namgoong, J. W.; Yuk, S. B.; Chung, S. W.; Kim, J. P. Simple Modification of Basic Dyes with Bulky & Symmetric WCAs for Improving Their Solubilities in Organic Solvents without Color Change. *Sci. Rep.* **2017**, *7*, 46178.

(39) Funabiki, K.; Yanagawa, R.; Kubota, Y.; Inuzuka, T. Thermo- and Photo-Stable Symmetrical Benzo[cd]indolenyl-substituted Heptamethine Cyanine Dye Carrying a Tetrakis(Pentafluorophenyl)Borate that Absorbs only Near-Infrared Light over 1000 nm. *New J. Chem.* **2019**, *43*, 7491–7501.

(40) Bates, M.; Lunt, R. R. Organic Salt Photovoltaics. *Sustain. Energy Fuels* **2017**, *1*, 955–968.

(41) Traverse, C. J.; Chen, P.; Lunt, R. R. Lifetime of Organic Salt Photovoltaics. *Adv. Energy Mater.* **2018**, *8*, 1703678.
(42) Young, M.; Suddard-Bangsund, J.; Patrick, T. J.; Pajares, N.; Traverse, C. J.; Barr, M. C.; Lunt, S. Y.; Lunt, R. R. Organic Heptamethine Salts for Photovoltaics and Detectors with Near-Infrared Photoresponse up to 1600 nm. *Adv. Opt. Mater.* **2016**, *4*, 1028–1033.
(43) Bouit, P. A.; Aronica, C.; Toupet, L.; Le Guennic, B.; Andraud, C.; Maury, O. Continuous Symmetry Breaking Induced by Ion Pairing Effect in Heptamethine Cyanine Dyes: Beyond the Cyanine Limit. *J. Am. Chem. Soc.* **2010**, *132*, 4328–4335.
(44) Tatikolov, A. S.; Dzhulibekov, K. S.; Shvedova, L. A.; Kuzmin, V. A.; Ishchenko, A. A. Influence of Inert Counterions on the Photochemistry of Some Cationic Polymethine Dyes. *J. Phys. Chem*. **1995**, *99*, 6525–6529.
(45) Kong, N. S.; Jung, H.; Kim, B.; Lee, C. K.; Kong, H.; Jun, K.; Kim, J. C.; Noh, S. M.; Cheong, I. W.; Park, J.; Il Park, Y. Development of Dimeric Triarylmethine Derivatives with Improved Thermal and Photo Stability for Color Filters. *Dyes Pigments* **2017**, *144*, 242–248.
(46) Reese, M. O.; Gevorgyan, S. A.; Jørgensen, M.; Bundgaard, E.; Kurtz, S. R.; Ginley, D. S.; Olson, D. C.; Lloyd, M. T.; Morvillo, P.; Katz, E. A.; Elschner, A.; Haillant, O.; Currier, T. R.; Shrotriya, V.; Hermenau, M.; Riede, M.; R. Kirov, K.; Trimmel, G.; Rath, T.; Inganäs, O.; Zhang, F.; Andersson, M.; Tvingstedt, K.; Lira-Cantu, M.; Laird, D.; McGuiness, C.; Gowrisanker, S. (Jimmy); Pannone, M.; Xiao, M.; Hauch, J.; Steim, R.; DeLongchamp, D. M.; Rösch, R.; Hoppe, H.; Espinosa, N.; Urbina, A.; Yaman-Uzunoglu, G.; Bonekamp, J.-B.; van Breemen, A. J. J. M.; Girotto, C.; Voroshazi, E.; Krebs, F. C. Consensus Stability Testing Protocols for Organic Photovoltaic Materials and Devices. *Sol. Energy Mater. Sol. Cells* **2011**, *95*, 1253–1267.
(47) Delley, B. An All-electron Numerical Method for Solving the Local Density Functional for Polyatomic Molecules. *J. Chem. Phys*. **1990**, *92*, 508–517.
(48) Perdew, J. P.; Wang, Y. Accurate and Simple Analytic Representation of the Electron-Gas Correlation Energy. *Phys. Rev. B* **1992**, *45*, 13244–13249.
(49) Ribeiro, T. C. da S.; Costa, R. F. da; Bezerra, E. M.; Freire, V. N.; Lyra, M. L.; Manzoni, V. The Quantum Biophysics of the Isoniazid Adduct NADH Binding to Its InhA Reductase Target. *New J. Chem.* **2014**, *38*, 2946–2957.
(50) Vianna, J. F.; Bezerra, K. S.; Oliveira, J. I. N.; Albuquerque, E. L.; Fulco, U. L. Binding Energies of the Drugs Capreomycin and Streptomycin in Complex with Tuberculosis Bacterial Ribosome Subunits. *Phys. Chem. Chem. Phys.* **2019**, *21*, 19192–19200.
(51) Dułak, M.; Wesołowski, T. A. Interaction Energies in Non-Covalently Bound Intermolecular Complexes Derived Using the Subsystem Formulation of Density Functional Theory. *J. Mol. Model.* **2007**, *13*, 631–642.
(52) Yang, C.; Liu, D.; Lunt, R. R. How to Accurately Report Transparent Luminescent Solar Concentrators. *Joule* **2019**, *3*, 2871–2876.

For Table of Contents Only